51st International Annual Conference of the Fraunhofer ICT
Cenvention Center, Gartenhalle, Karlsruhe, Germany, June 28- July 1, 2022

ADN solid propellants with high burning rates

Stefan Sims, Sebastian Fischer, Claudio Tagliabue
Fraunhofer Institute for Chemical Technology ICT
Pfinztal, Germany

Abstract

Modern solid propellants based on ammonium dinitramide (ADN) and Glycidyl Azide Polymer (GAP) have significant advantages in terms of environmental compatibility and thermodynamic performance. In the present work, it is shown that the already high burning rate of ADN solid propellants can be more than doubled by means of metallic fibres, which significantly increases the thrust of such engines. In order to achieve such results, 3 *wt%* of Al-Mg alloy fibres are added to the propellant. A formulation with 3 *mm* long fibres shows the highest burning rate with 84.0 *mm/s* at 26.5 *MPa*. Small scale motor tests confirm these investigations. The burning mechanism is studied by SEM/EDX investigations and by measuring the thermal conductivity. These show that the fibres remain on the burning surface and thus transfer the heat from the flame to the depth of the propellant. The thermal conductivity of samples with AlMg5 fibers is about 22 % higher than the reference.

Introduction

Solid rocket propellants are widely used propulsion systems in military and civil applications. The State-of-the-Art are composite propellants based on ammonium perchlorate (AP) as oxidizer, aluminum (Al) as fuel and hydroxyterminated polybutadiene (HTPB) as binder matrix. These formulations have been known and studied in detail for decades.
Due to increasing environmental awareness, alternative oxidizers have been under examination to replace AP, as this produces hydrochloric acid during combustion, among other negative properties like health hazards and intense exhaust plumes.
The most promising candidate is Ammonium dinitramide (ADN) in combination with Glycidyl Azide Polymer (GAP) as binder. This halogen-free oxidizer offers numerous advantages compared to AP, such as higher specific impulse and reduced signature, in addition to a lower environmental impact [1, 2].

Concerning ADN-based solid rocket propellants, some significant differences to AP-based propellants are known; unlike AP the burning rate of ammonium dinitramide increases with larger particle size [3]. Apart from this, there are only a few possibilities of catalysts described in the literature. Korobeinichev et al. reported that the regression rate of ADN can be decreased by CuO and Cu_2O [5]. Furthermore, substitution of ADN or GAP by low-energy substances can also lower the burning rate, because of a reduction in the heat of combustion [4-6].

The need of high burning rate propellants has been growing in recent years, driven not least by further interest and developments in hypersonic technologies.
Hypersonic missiles with a RAM-jet or SCRAM-jet engine require to be accelerated to supersonic speed by a carrier rocket in order to generate thrust efficiently. These boosters normally use conventional chemical propulsion systems based on AP/HTPB/Al.

In addition to the previously discussed environmental awareness, booster materials that promise even greater acceleration are being sought for this application. On the one hand, this can be achieved by a grain geometry that offers a larger burning surface and thus increases the mass flow. Complicated geometries such as wagon-wheel burners or star burners are available for this purpose, but they can be problematic to manufacture. On the other hand, fast-burning propellants can keep the geometry simple, e.g. a end- or tub-burner. This has the advantage that the required volume of the motor can be kept small, which also leads to a benefit in the structural mass and aerodynamic drag.

For AP-propellants the regression rate can be increased by using fine particles with $d_{50} < 5$ *μm* [7]. As the literature does not indicate any possibilities of significantly increasing the burning rate of ADN propellants by chemical modification, other ways must be found.

Another known possibility to increase the burning rate are embedded metallic wires with the aim to increase the thermal conductivity of the propellant. Examples are given at least at the field of gas generators [8, 9]. Moreover Friedman et al. and Glick et al. investigated embedded wires in the late 1960's [10, 11]. Since then, numerous publications report about the behavior of embedded wires in composite and double base propellants [12-18].

Nevertheless, embedded wires are not reported in ADN composite propellants so far, because ADN has some important different properties and peculiarities in comparison to AP or AN. Menke et al. report about the reaction behavior of Ammonium dinitramide with isocyanates and how to suppress it for curing [19]. Furthermore, the combustion behavior of ADN propellants follows other decomposition mechanisms and some known catalytic materials from AP propellants, like Iron Oxide, simply do not show an effect in ADN analogue, as Tagliabue et al. reported [20, 21]. Besides, ADN and/or GAP are very reactive with common ballistic modifiers like Benzoylferrocene, ZnO, MgO and show incompatibilities issues [21].

This multitude of different properties means that ADN must be considered in a separate manner from other oxidizers and knowledge cannot simply be transferred.

Experimental Section

Materials and preparation of propellants

The following table lists the used materials, their main specifications and their suppliers.

Tab. 1: Used materials

Compound	Specification	Supplier
prilled ADN	x_{50} = 103 *μm*	Eurenco Bofors
GAP-diol	EQ = 1250 *g/mol*	Eurenco France
HTPB R45M	EQ = 1300 *g/mol*	Total Petrochemicals
Tolonate HDT-LV2	EQ = 183 *g/mol*	Vencorex
Baymedix AP501	EQ = 328 g/mol	Covestro
DBTL	Purity min. 98 %	abcr
AlMg5 fibers	L = 0.5, 1, 3 *mm* ø90 *μm*	Deutsches Metallfaserwerk
Al X-81	x_{50} = 23 *μm*	Toyal America
Mg	x_{50} = 44 *μm*	Alfa Aesar
AlMg5 particles	x_{50} = 21 *μm*	Toyal Europe

The AlMg5 fibers are named after their length:

- 0.5 *mm* = M05
- 1.0 *mm* = M1
- 3.0 *mm* = M3

All compounds are mixed with a contactless planetary centrifugal mixer from Thinky, model ARV-310, and casted into teflonized molds with geometry 150x45x8 *mm (LxWxH)*. All samples are cured for 7 days at 40 °C.
At this point, it must be noted that the AlMg5 M3 fibers are very demanding in processing. In order to obtain homogeneous mixtures, it is not possible to add one solid fraction after the other, as is usually done, but to add them step by step. Thus, after the GAP-diol, a part of the ADN is added to the fibers and mixed with 2000 rounds per minute. This is followed by a second ADN fraction, which is processed at moderate speeds about 1600 rounds per minute in the Thinky Mixer. The mixture obtained is visually evaluated and, if necessary, an additional mixing step is carried out to achieve a satisfactory mixing result.

The following propellants were investigated:

Tab. 2: Propellant Samples

Sample No.	Binder [wt%]	ADN [wt%]	BM [wt%]
S1 (reference)	30 (GAP)	70	-
S2	30 (GAP)	67	2.85 Al + 0.15 Mg
S3	30 (GAP)	67	3 (AlMg5 Powder)
S4	30 (HTPB)	67	3 (AlMg5 M1)
S5	30 (GAP)	67	3 (AlMg5 M05)
S6	30 (GAP)	67	3 (AlMg5 M1)
S7	30 (GAP)	67	3 (AlMg5 M3)
S8	30 (HTPB)	70	-

Burning rate measurement

The samples were cut into strands of 150x5x5 *mm* and coated with FlexCoat™ Rapid polyurea inhibition by dip-coating. The linear burning rate is determined at 25 *°C* in the pressure range of 7 to 26.5 *MPa* in a Crawford bomb in quasi-constant pressure state with an inert nitrogen atmosphere [22]. Each data point is the average of at least two measurements. If the standard deviation of these two measurements is > 5 %, a second duplicate measurement is added, so that the shown datapoint is the average of four measurements.

Interrupted combustion tests/SEM

To assess the burned surface, an interrupted combustion test was performed. For this purpose, a hanging strand is burnt off at 0.1 to 0.2 *MPa* in an optical window bomb. After about 5 *mm*, a holding wire is burned through, causing the remaining propellant to fall into a tank filled with liquid nitrogen. The sudden cooling causes the sample to extinguish, and it can be examined in detail.
The extinguished propellant surfaces is investigated by scanning electron microscopy (SEM). Therefore, the sample is first sputtered with gold and then examined in the Zeiss Supra 55VP with a coupled EDAX Genisis 4000 EDX.

Thermal conductivity

For thermal conductivity investigation, a THB 100 from Linseis, which employs the Transient Hot Bridge method, is used. The test is performed at 25 *°C*.

Small scale motor test

In order to investigate the burning behavior under conditions closer to the real application, small scale motor tests were carried out. Due to the required propellant mass, these samples were produced in a planetary mixer from IKA, model HKV5. The order of addition of the individual components was identical to the preparation in the Thinky Mixer. Approx. 320 *g* of the propellant was casted directly into a steel cartridge, the inner surface of cartridge was prior treated with plasma to ensure the best possible adhesion of the propellant. An end burner configuration (65 *mm* in diameter and 60 *mm* in heights) was chosen as grain geometry. The propellant loaded cartridge, which enables a quick change of the samples due to its modularity, is then placed in the test motor.
The test motor is designed in "Battleship configuration" with 8 *mm* wall thickness and heavy construction to absorb unexpected pressure peaks as much as possible.
In order to investigate the quality of the produced propellants, computerized tomography imaging was performed with a Bruker SkyScan 2211 Multisclae X-ray nanotomograph with a X-ray source, model XWT-1060-TC from X-Ray WorX, and detector CMOS-Flat-Panel, model DT-001009 from Varex Imaging. Scan parameters are set to 120 *kV* X-ray source and 80 *µA* of current while using an 0.5 *mm* aluminium filter. Furthermore, image resolution is 25 *µm/px*, shutter speed is 400 *ms* and rotation step width of 0.15° is used.

A pressure transducer is attached to the test motor, which measures the combustion chamber pressure during firing. The motor itself is mounted on an horizontal carriage and a push rod transmits the generated thrust to a 2 *kN* pressure sensor. Using the burn rates obtained from the Crawford, the chamber pressure can be calculated, knowing the nozzle diameter. A target pressure of 10 *MPa* is usually set but since the nozzle geometries are available only in limited steps, it is not always achievable. A mixture of boron and potassium nitrate (B/KNO_3) with a coarse particle distribution within 1-2 *mm* is used to ignite the ADN/GAP propellants. Since these propellants tend to crack and subsequently burst a low igniter charge density is employed (0,02 g/cm^3).

The reference ADN/GAP (S1), ADN/GAP/Al/Mg (S2) and ADN/GAP/AlMg5 M1 (S6) were investigated at 25 °C.
For the evaluation of the average pressure and thrust, the inflection points of the graphs are used to define the limits. For better comparability, the burning rate from the Crawford measurements is calculated using Vieille's law (equation 1) on the averaged motor pressure in order to compare the burning rates at the same pressure [23].

$$r_b = a \cdot p^n \quad (1)$$

Results and Discussion

Burning behavior

Linear burning rate

The following results refer to Crawford measurements.
Masafumi and Kenji report about a dependency of the burning rate from both length and width of the used wires [24]. In the presented work only the length is considered with a constant diameter of 90 *µm*.

The fibers are an alloy of 95 *wt%* aluminium and 5 *wt%* magnesium. Figure 1 shows the burning rates of ADN/GAP propellants where the burning rate modifiers Al and Mg are embedded as a separate particle mixture (ADN/GAP/Al/Mg; S2) as alloy powder (ADN/GAP/AlMg5; S3) and as alloy fibers (ADN/GAP/AlMg5 M1; S6). Thus, the chemical composition of these propellants is the same, only the particle modification differs.

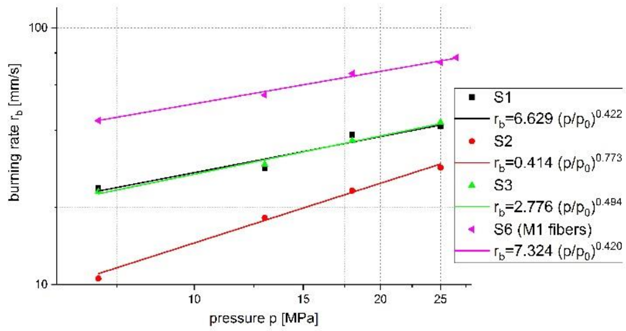

Fig. 1: Linear burning rate of ADN/GAP (S1) black, ADN/GAP/Al/Mg (S2) red, ADN/GAP/AlMg5 (S3) green, ADN/GAP/AlMg5 M1 (S6) pink

The graphic shows negligible difference between the AlMg5 powder and the reference, just a slightly higher-pressure exponent. The mixture of Al and Mg particles (S2) decreases the burning rate drastically with a simultaneous increase of the pressure exponent up to 0.773, which leads to an unsafe handling in practical applications. Indeed, a pressure exponent of 0.5 or lower is usually required. The AlMg5 M1 fibers nearly doubles the burning rate of the ADN/GAP propellant up to 76.3 *mm/s* at 26.5 *MPa*.

The measurements show that the chemical composition of the burning rate modifier has little to no influence on the regression rate, except the mixture Al + Mg. This decreasing effect needs to be investigated in further studies. The accelerating effect can only be detected with the fibers. This led to the assumption that the heat transfer to the depth of the propellant is significantly increased. Thus, the condensed phase is quickly heated, and the decomposition of the ADN is initiated earlier, leading to the high burning rates.

Based on the previous experience, fibers with a length of 0.5 *mm* and 3.0 *mm* are also examined, and the outcome is shown in Figure 2.

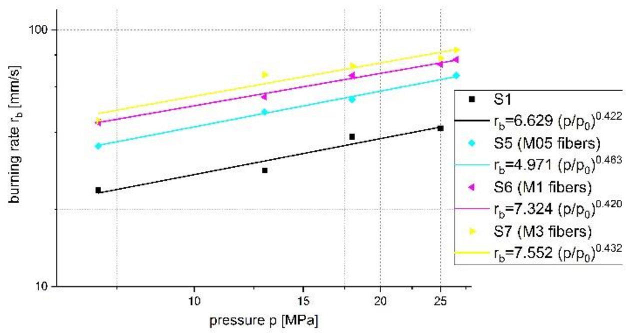

Fig. 2: Linear burning rate of ADN/GAP (S1) black, ADN/GAP/AlMg5 M05 (S5) turquoise, ADN/GAP/AlMg5 M1 (S6) pink, ADN/GAP/AlMg5 M3 (S7) yellow

The results show a clear dependence of the burning rate on the fiber length. The smallest influence is exerted by 0.5 *mm* long fibers, the largest by those of 3.0 *mm*. The pressure exponent of all propellants remains almost unchanged in the range 0.43 to 0.46. The maximum r_b of 84.0 *mm/s* is reached by the M3 fibers at 26.5 *MPa*.

In order to investigate the effectiveness of the burning rate moderator in other propellant systems, the burning rate of an ADN/HTPB propellant with and without M1 fibers was also measured in the Crawford bomb. The results are shown in Figure 3.

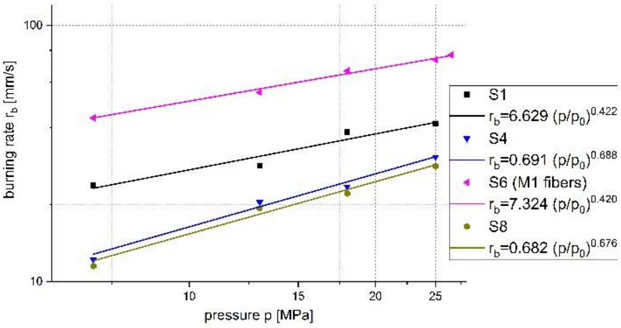

Fig. 3: Linear burning rate of ADN/GAP (S1) black, ADN/HTPB/AlMg5 M1 (S4) blue, ADN/GAP/AlMg5 M1 (S6) pink, ADN/HTPB (S8) brown

Surprisingly, the effect of the BM does not appear in the low-energy system ADN/HTPB. Here, the usual decrease of the burning rate due to substitution with inert components in the propellant can be observed, as described by Korobeinichev et al. [5,6].

Furthermore, a significantly higher pressure exponent for both samples S4 and S8 can be noticed, which can be attributed to the different burning behavior of ADN/HTPB propellants.

Further work should address this phenomenon, because the effect of the fibers only occurs in a GAP-based system. In order to support this thesis, a GAP-based propellant with AP or AN must be examined.

Interrupted combustion and SEM/EDX mapping

The interrupted combustion tests were difficult to carry out due to the high burning rate of the propellants. Indeed, the samples often continued to burn during the fall into the liquid nitrogen container, so no propellant remains without temperature effect. This can be seen very well in the formation of voids in the propellant due to decomposed ADN. For this reason, the investigations had be carried out close to the pressure deflagration limit (PDL), which, for ADN/GAP propellants, is around 0.1 *MPa*.

The SEM images of the burned surface of reference S1 show clearly visible hemispheres in the binder matrix compared to the unburned sample (Figure 4).

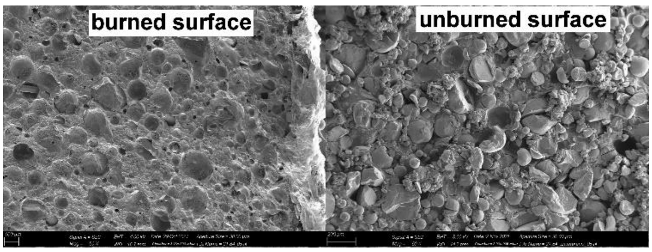

Fig. 4: SEM images of ADN/GAP propellant (S1), burned surface (left), unburned surface (right)

Simultaneously, EDX mapping measurements were taken from the burned and unburned surface. The plot in Figure 5 shows the elements carbon (red), nitrogen (green) and oxygen (blue) next to the SEM image (grey).

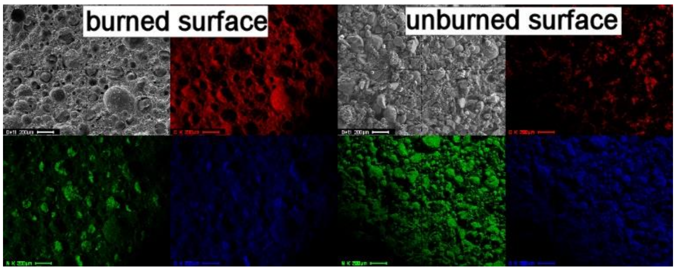

Fig. 5: EDX mapping of ADN/GAP (S1) formulation

The following table shows the measured atomic concentrations on the sample surface of S1.

Tab. 3: EDX analysis of unburned/ burned surface of S1

Element	Unburned	Burned
Carbon [wt%]	15.16	39.12
Nitrogen [wt%]	46.48	32.48
Oxygen [wt%]	36.14	24.89
Aluminum [wt%]	n.a.	0.03
Magnesium [wt%]	n.a.	0.03

After combustion, the content of nitrogen and oxygen decreases on the surface while carbon is enriched.

In addition to the mentioned voids in the propellant, a larger residue of nitrogen after burning was unexpectedly observed but. This can possibly be attributed to the melting and initial decomposition of ADN at the burning surface. Korobeinichev et al. described this as well: during the combustion of ADN/GAP propellants, the ADN first dissociates into ammonia (NH_3) and dinitramic acid (HN_3O_4) [25]. Fogelzang et al. similarly assumed that ADN combusts at a lower temperature than GAP [26].

This leads to the assumption, that ADN decomposes near the surface and forms condensed species, e.g. nitric acid and its clusters and ammonium nitrate, like Lang and Bohn reported for the decomposition of pure ammonium dinitramide [27]. However, the detailed decomposition pathway for an ADN propellant is not fully investigated yet.

Comparative burning interruptions of ADN/GAP propellants with AlMg5 fibers were carried out. Despite the different fiber lengths, the results are almost identical, so for better illustration only M3 fibers are discussed.

Figure 6 compares SEM images of the burnt surface of the sample S7 (left) with an unburned surface (right).

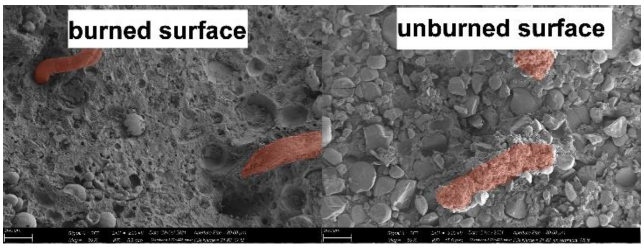

Fig. 6: SEM images of ADN/GAP/AlMg5 M3 propellants, burned surface (left) and unburned surface (right), fibers marked in red

It is notable that on the unburned sample, the M3 fibers are fully covered with ADN particles, which can be identified by their needle shapes. Thus, the metal fibers can transfer the generated heat during decomposition very efficiently into the depth of the propellant. This is confirmed by the image of the burned surface, where the fibers are exposed. Furthermore, the burning surface shows the known voids in the binder matrix caused by decomposed ADN. Like the examination of the S1 propellant, Figure 7 shows the EDX mapping of the ADN/GAP/AlMg5 M3 propellant. For better understanding, aluminium (purple) is chosen instead of oxygen to represent the fiber material. The EDX measurements are shown in table 4.

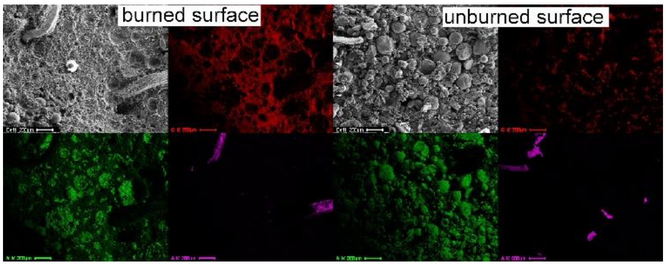

Fig. 7: EDX mapping of ADN/GAP/AlMg5 M3 (S7) formulation

Tab. 4: EDX analysis of unburned/ burned surface of S7

Element	Unburned	Burned
Carbon [wt%]	17.45	32.23
Nitrogen [wt%]	47.38	26.74
Oxygen [wt%]	31.43	28.01
Aluminum [wt%]	1.49	0.61
Magnesium [wt%]	0.12	0.04

The EDX mapping confirmed the results of the SEM images: the exposed AlMg5 fibers can be clearly seen. After decomposition, nitrogen and oxygen decreases on the surface while carbon increases, which is the same behavior like S1.

Comparing the burned sample of S1 with S7, the nitrogen content of the latter is 5.74 *wt%* lower, which indicates a fast decomposition of ADN. The higher amount of oxygen of the burned S7 sample refers to the formation of Al_2O_3.

The results of the interrupted combustion tests suggest that the fiber materials remain on the burning surface and extend into the gaseous phase of the flame. Thus, an increased heat transfer into the propellant takes place.

Investigation of the thermal and thermochemical properties of the propellants can offer conclusions about the mechanism of the burning rate modifiers.

Small scale motor test

Each cartridge was examined via CT, with exemplary sample S6 being illustrated. Figure 8 shows a 3D image of the cylindrical sample, whereby the coloring was adapted to the density of the material in order to emphasize the fibers´ orientation. The AlMg5 M1 are shown in red. The sectional view (right) indicates two accumulations of fibers above and below the center of the sample, which will have an influence on the burning behavior in the motor test. However, no preferred orientation of the fibers is evident, which should eliminate the dependence on fiber orientation.

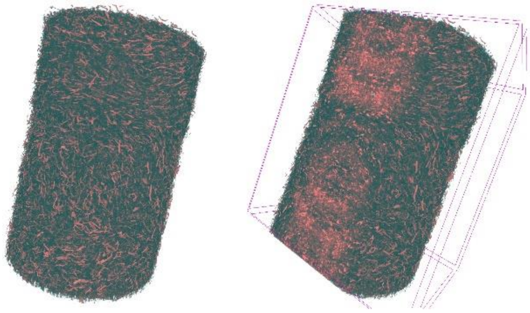

Fig. 8: Computer tomography imaging of S6, AlMg5 M1 fibers in red

The small-scale motor tests were all successful. Due to the soft ignition and the sufficiently homogeneous distribution of the solid particles, all propellants show a constant pressure level. As expected, no primary signature was observed with formulation S1 (ADN/GAP), as it does not form condensed combustion products. On the other hand, samples S2 and S6 show slight smoke due to the formed metal oxides. Table 5 shows the results of the motor tests.

Tab. 5: Small scale motor test of ADN/GAP/BM formulations

No.	avg. Thrust [N]	avg. pressure [MPa]	burning time [s]	r_b motor [mm/s]	r_b Crawford [mm/s]	r_b deviation [%]
S1	356.2	10.41	1.98	30.42	29.28	-3,7
S2	321.6	8.46	2.26	26.50	24.08	-9.13
S6	500.3	8.14	1.36	44.08	46.46	5.40

The AlMg5 M1 fibers also show the accelerating effect in the motor as they did in the Crawford measurements.

Despite 2.3 *MPa* less in the chamber, the burning rate of the sample with M1 fibers is 13.7 *mm/s* faster (44.1 *mm/s*) than the ADN/GAP propellant by 10 *MPa*, which corresponds to an increase of approx. 45 %.

The decreasing effect on the burning rate of the particle mixture Al + Mg (S2) is confirmed by the motor test. Nevertheless, further research on this behavior needs to be done, especially considering that Biswas and Vellaisamy reported an opposite effect for AP-based propellants [28].

It is noticeable that the burning rate of sample S6 with fibers in the motor is slower than the corresponding calculated value from the Crawford measurement. In contrast, samples S1 and S2 show a higher burning rate. Sutton and Biblarz report about higher burning rates in small-scale motors compared with strand burners because of differences in the temperature of the hot chamber environment [29].

The lower burning rate of S6 of the motor test compared with its Crawford results has to be investigated in further studies. Once the orientation and accumulation of the used AlMg5 M1 fibers may lead to slightly different burning behaviors in terms of thermal conductivity into the depth of the propellant. This will have an influence on the preheating of the sample and will expressed in different burning rates.

Thermal conductivity

The interrupted combustion tests indicate that the fiber materials remain at the burning surface and protrude into the flame, allowing the heat of combustion to be conducted into the depth of the propellant via the AlMg5 fiber. To further investigate this assumption the thermal conductivity is examined.

The thermal conductivity of ADN/GAP propellants with different burning rate modifiers are investigated by hot bridge method. The results are shown in Table 6.

Tab. 6: Thermal conductivity of ADN/GAP propellants

Sample	Formulation	Thermal conductivity [W/m·K]
S1	ADN/GAP	0.341
S2	ADN/GAP/Al/Mg	0.332
S6	ADN/GAP/AlMg5 M1	0.417
S7	ADN/GAP/AlMg5 M3	0.417

The results are in agreement with the assumpions suggested by the SEM investigations. The thermal conductivity of ADN/GAP propellants can be increased for approx. 22 % by adding AlMg5 fibers. However, the thermal conductivity is not dependent on the fiber length. This length independence is achieved by a homogeneous distribution of the fibers in the propellant, where the individual fibers partly touch each other and thus act as bridges.

It is interesting to note that the addition of individual aluminum and magnesium particles does not increase the thermal conductivity. This can lead to the conclusion that the metal particles are insulated by the GAP binder.

Conclusion

The burning rate of ADN/GAP propellants with metallic fiber materials and their mechanism of functioning are investigated. By using AlMg5 fibers, the burning rate can be more than doubled. There is a clear dependence on the fiber length, with longer fibers resulting in higher burning rates. A maximum of 84.0 *mm/s* at 26.5 *MPa* is reached with 3 *mm* long AlMg5 fibers. It can be demonstrated that this increase is not achieved by particulate BMs despite the chemically identical composition. However, the effect of the fibers is only evident in the ADN/GAP system. This isn´t shown in the low-energy system ADN/HTPB. Furthermore, the accelerating effect of the fiber materials can be demonstrated in small scale motor tests.

The causes of the effect was investigated by using interrupted combustion tests with subsequent SEM examination as well as by measurement of the thermal conductivity. It was shown that the fibers remain above the burning surface during combustion and protrude into the flame. Due to the increased thermal conductivity, the heat of combustion can be transferred deeper into the propellant, which leads to a higher decomposition rate.

Symbols and Abbreviations

ADN	Ammonium dinitramide
AlMg5	Alloy of 95 *wt%* aluminum +5 *wt%* magnesium
AP	Ammonium perchlorate
BM	Burning rate modifier
CT	Computer Tomography
DBTL	Dibutyltindilaurate

DSC	Differential Scanning Calorimetry
EDX	Energy-dispersive X-ray spectroscopy
GAP	Glycidyl Azide Polymer
HTPB	Hydroxyl-terminated polybutadiene
p_0	Atmospheric pressure (0.1 *MPa)*
SEM	Scanning electron microscopy
$Q_{dec.}$	Specific Heat of decomposition
$T_{dec.}$	Decomposition temperature
T_m	Melting temperature
v_0	Starting velocity of a Ramjet

Acknowledgements

Numerous employees of the Fraunhofer ICT contributed to this work. The authors would like to thank all colleagues of the Solid Propellants and Explosives Research Group. Furthermore, to Andreas Imiolek and Diana Bieroth for performing the combustion investigations, Dr. Mar Juez-Lorenzo and Claudia Seidel for the SEM investigations, and Kathrin Henning for the thermal conductivity measurements.

The authors also want to thank the German Ministry of Defence for financial support.

References

[1] P. Kumar, An overview on properties, thermal decomposition, and combustion behavior of ADN and ADN based solid propellants, *Def. Technol.* **2018,** 14, 661-673

[2] L.T. DeLuca, I. Palmucci, A. Franzin, V. Weiser, V. Gettwert, N. Wingborg, M. Sjöblom, New Energetic Ingredients for Solid Rocket Propulsion, *Guti Huojian Jishu/Journal of Solid Rocket Technology* **2016**, 39, 6, 765-774

[3] Z. Pak, Some ways to higher environmental safety of solid rocket propellant application, *AIAA/SAE/ASME/ASEE 29th Joint Propulsion Conference and Exhibit*, June 28-30, **1993,** Montery, CA, USA, AIAA-93-1755

[4] W. Pang, X. Fan, W. Zhang, H. Xu, S. Wu, F. Liu, W. Xie, N. Yan, Effect of Ammonium Dinitramide (ADN) on the Characteristics of Hydroxyl Terminated Polybutadiene (HTPB) Based Composite Solid Propellant, *J. Chem. Sci. Technol.* **2013**, 2, 2, 53-60

[5] O.P. Korobeinichev, A.A. Paletskii, A.G. Tereschenko, E.N. Volkov, Combustion of ammonium dinitramide/polycaprolactone propellants, *Proc. Combust. Inst.* **2002**, 29, 2955-2961

[6] O.P. Korobeinichev, A.A. Paletskii, Flame Structure of ADN/HTPB Composite Propellants, *Combust. Flame* **2001**, 127, 3, 2059-2065

[7] X., Guo, F. Li, H. Song, G. Liu, L. Kong, M. Li, Combustion Characteristics of a Novel Grain-Binding High Burning Rate Propellant, *Propellants, Explos., Pyrotech.* **2008**, 33, 4, 255-260

[8] C.H. Jackson Jr., *Gas Generating Compositions*, US Patent 4,386,979, Morgan Hill, CA, USA, **1983**

[9] R.D. Taylor, T.M. Deppert, *Gas Generant Composition for use with Aluminum Components*, US Patent 5,529,647, Brigham City, UT, USA, **1996**

[10] R. Friedman, R.G. Nugent, K.E. Rumbel, A.C. Scurlock, Deflagration of ammonium perchlorate, *Symposium (International) on Combustion* **1966**, 6(1), 612-618

[11] L.H. Caveny, R.L. Glick, Influence of Embedded Metal Fibers on Solid-Propellant Burning Rate, *J. Spacecr.* **1967**, 4, 79-85

[12] S. Isert, C.D. Lane, I.E. Gunduz, S.F. Son, Tailoring burning rates using reactive wires in composite solid rocket propellants, *Proc. Combust. Inst.* **2017**, 36 (2), 2283-2290

[13] L.J. Hurt, *The Study of the Mechanism of Enhanced Burning Rate of Solid Propellants*, Report No. S-45, Rohm & Haas Company, Huntsville, AL, USA **1964**

[14] P. C. Winch, R. D. Irvine, Active Control of Solid Propellant Consumption Rate by Forced Cone Burning, *J. Propul. Power* **1988**, 4, 104-110

[15] N.N. Bakhman, I.N. Lobanov, Influence of the Diameter of the Heat-Conducting Elements on their Efficiency During the Combustion of Condensed Systems, *Combust. Explos. Shock* **1983**, 9, 42-46

[16] N. Kubota, M. Ichida, T. Fujisawa, Combustion Processes of Propellants with Embedded Metal Wires, *AIAA J.* **1982**, 20, 116-121

[17] K. E. Rumbel, Poly(vinyl chloride) Plastisol Propellants in: *Propellants Manufacture, Hazards, and Testing* (Eds.: C. Boyars, K. Kalger), American Chemical Society, Washington DC **1969**, pp. 36-66

[18] C. Shuling, L. Fengsheng, Influence of Long Metal Wires on Combustion of Double-Base Propellants, *Combust. Flame* **1982**, 45, 213-218

[19] K. Menke, T. Heintz, W. Schweikert, T. Keicher, H. Krause, Formulation and Properties of ADN/GAP Propellants, *Propellants, Explos., Pyrotech.* **2009**, 34, 218-230

[20] T.B. Brill, P.J. Brush, D.G. Patil, Thermal decomposition of energetic materials 58. Chemistry of ammonium nitrate and ammonium dinitramide near the burning surface temperature, *Combust. Flame* **1993**, 92(1-2), 178-186

[21] C. Tagliabue, V. Weiser, A. Imiolek, M.A. Bohn, T. Heintz, V. Gettwert, Burning Behavior of AN/ADN Propellants, *48th International Annual Conference of the Fraunhofer ICT- Reactivity and Modelling*, June 27-30, **2017**, Karlsruhe, Germany, P107

[22] R.G. Parr, B.L. Crawford, A physical theory of burning of double-base rocket propellants I, *J. Phys. Colloid Chem.* **1950**, 54, 929-954

[23] N. Kubota, *Propellants and Explosives*, 3rd revised and updated Edition, Wiley-VCH, Weinheim **2015**, p. 17

[24] T. Masafumi, M. Kenji, Burning rate increment of solid propellant with embedded metal wires in a bundle, *Explosion and Explosives* **1991**, 52 (4), 270 – 277

[25] L.V. Kuibida, O.P. Korobeinichev, A.G. Shmakov, E.N. Volkov, A.A. Paletsky, Mass Spectrometric Study of Combustion of GAP- and ADN-based Propellants, *Combust. Flame* **2001**, 126, 3, 1655-1661

[26] A.E. Fogelzang, V.P. Stinditskii, V.Y. Egroshev, A.I. Levshenkov, V.V. Serushkin, V.I. Kolesov, Combustion behavior and flame structure of ammonium dinitramide, *28th International Annual Conference of ICT*, June 24–27, **1997**, Karlsruhe, Germany, 1–14.

[27] J. Lang, M.A. Bohn, Decomposition Pathways of Ammonium Dinitramide (ADN) and its HNO3-ClustersElucidatedby DFT-Calculations, *Propellants, Explos., Pyrotech.* **2021,** 46, 233-244

[28] U. Vellaisamy, S. Biswas, Effect of metal additives on neutralization and characteristics of AP/HTPB solid propellants, *Combust. Flame* **2020**, 221, 326-337

[29] G.P. Sutton, O. Biblarz, *Rocket Propulsion Elements*, 7th Edition, John Wiley & Sons, New York **2001**, p. 427